Theory of electron spin resonance in Haldane-gap antiferromagnets

Ian Affleck
Canadian Institute for Advanced Research and Physics Department, University of British Columbia, Vancouver, British Columbia, Canada V6T 1Z1
(Received 2 January 1992)

Recent electron-spin-resonance experiments on the one-dimensional Heisenberg antiferromagnet, NENP, have observed 47-GHz transitions in magnetic fields of 1.4–5 T, depending on orientation. We argue that these should be understood as transitions between magnon states of a wave vector near π and different polarizations, whose energies are split by crystal-field anisotropy and magnetic fields. Neutron scattering measurements and/or models of the magnon spectrum thus determine the ESR resonance frequencies.

Integer-spin Heisenberg antiferromagnetic chains have a singlet groundstate and a gap to the lowest excited state, a triplet, as was first argued by Haldane.[1] Experimental evidence for the Haldane gap was first obtained by Buyers *et al.*[2] in $CSNiC_3$. However a much more one-dimensional system was studied later,[3] $Ni(C_2H_8N_2)_2NO_2(ClO_4)$ (NENP). It has an exchange energy of about 47 K and exhibits no Néel order down to 1.2 K due to the tiny ratio of interchain to intrachain couplings (≈ 0.0006). Neutron-scattering experiments exhibit three different branches of magnons, with minimum energy at wave vector π (we set the lattice spacing to one) and energies 2.52, 1.34, and 1.17 meV.

More recently, electron-spin-resonance (ESR) experiments have been performed on NENP.[4] These exhibited a thermally activated resonance at a frequency of 47 GHz or 0.19 meV in magnetic fields of 1.4–5 T depending on orientation. [These experiments were performed on pure samples and are not to be confused with the ones performed[5] on doped samples, which probe lower energy degrees of freedom at the ends of finite chains.] Note that this transition energy is close to the energy difference between the two lowest magnons. In this paper we argue that the ESR experiments should be interpreted in terms of transitions between magnon states. Thus it is not necessary to postulate some additional excitations, as was done in Ref. 4. Indeed it would be difficult to understand why these additional excitations have not been seen in other experiments or numerical simulations. Instead the ESR transition frequencies can be determined from neutron-scattering data. Recent neutron-scattering experiments at finite field[6] are in excellent agreement with the ESR data for one field orientation. Adopting models for the field (and wave vector) dependent magnon energies, which agree quite well with all existing neutron-scattering data, allows us to predict the ESR transition frequencies at all field orientations in reasonable agreement with experiment. Further neutron-scattering experiments could test this picture. The models are also used to calculate the width and temperature dependence of the resonance. In the isotropic case the resonance is a δ function but it is broadened by crystal-field anisotropy. However, the models predicts a considerably narrower resonance than seen experimentally. The temperature dependence is predicted to be essentially exponential in the (lowest) Haldane gap.

The ESR power absorption is proportional to the imaginary part of the susceptibility $I(\omega) \propto \omega \chi''(\omega)$; where

$$2\hbar\chi''(\omega) = (1 - e^{-\hbar\omega/T}) \int_{-\infty}^{\infty} dt\, e^{i\omega t} \langle \mathcal{S}^x(t) \mathcal{S}^x(0) \rangle_T , \quad (1)$$

where we assume the microwave field is polarized in the x direction, $\mathcal{S}^a$ is the total spin operator

$$\mathcal{S}^a = \sum_i S_i^a , \quad (2)$$

and the sum runs over all spins on the chain. $\chi''(\omega)$ is an odd function of ω so we henceforth assume $\omega > 0$. Let us first consider the case of an isotropic Haldane-gap antiferromagnet. The groundstate is a singlet and the lowest excitation is a triplet with a dispersion relation of the form

$$E(k) \approx \Delta + v^2 (k - \pi)^2 / 2\Delta + \cdots . \quad (3)$$

The next-lowest excitation after the single magnon is the two-magnon continuum beginning at $E = 2\Delta$ (and $k = 0$). [This field-theory prediction is confirmed by numerical simulations.[7]] Thus at temperatures $T \ll \Delta$, we may ignore all excitations except for the single magnon. We now consider a weak magnetic field, applied in the z direction with $0 < g\mu_B H \ll \Delta$. The effect on the dispersion of the triplet is to produce a standard Zeeman splitting:

$$\begin{aligned} E_z(k) &= E(k) , \\ E_{\pm}(k) &= E(k) \pm g\mu_G H . \end{aligned} \quad (4)$$

Note that this result is exact in the isotropic limit. Here z labels the magnon of total spin quantum number $\mathcal{S}^z = 0$ corresponding to fluctuations of the staggered magnetization in the z direction and $\pm$ label the magnons of total spin quantum number $\mathcal{S}^z = \pm 1$ corresponding to linear combinations of fluctuations of the staggered magnetization in the x and y directions. The matrix elements of the

total spin operator $\mathcal{S}^a$ between elements of the triplet are determined by rotational symmetry to be the same as for a single spin-one operator, for all wave vectors. Thus the ESR intensity is only nonzero when $\omega\hbar = g\mu_B H$ and

$$2\hbar\chi''\omega = L2\pi\hbar\delta(\omega\hbar - g\mu_B H) \times \sinh(\omega\hbar/T)\int (dk/2\pi)e^{-E(k)/T}, \quad (5)$$

where L is the length of the chain. At low T, the integral is dominated by $k \approx \pi$ and we find

$$2\hbar\chi''(\omega) = L\hbar\delta(\omega\hbar - g\mu_B H) \times \sinh(\omega\hbar/T)e^{-\Delta/T}\sqrt{2\pi\Delta T/v^2}. \quad (6)$$

Note that the resonance has zero width because the Zeeman splitting is the same for all wave vectors. At low temperatures the main contribution comes from almost stationary magnons with wave vector $(k-\pi)$ of $O(\sqrt{\Delta T}/v)$.

Let us now consider the effect of anisotropy. A crystal-field term $D\sum_i (S_i^z)^2$ splits the z mode from the + and − modes. A crystal-field term $E\sum_i[(S_i^x)^2-(S_i^y)^2]$ further splits the doublet. The field dependence of the dispersion relation of the three magnon branches is no longer determined by symmetry considerations alone; it becomes model dependent. In the ESR experiment, the static field was applied in the xy plane and the microwave field in the z direction. We denote the zero field $k=\pi$ magnons with energies 2.52, 1.34, and 1.17 meV as z, x and y, respectively, as in Ref. 6. The correspondence with crystallographic notation for NENP is $z=b$, $x=c$, and $y=a$. Upon the application of a magnetic field these three modes mix (i.e., they are no longer associated with a definite polarization of staggered magnetization fluctuations) and their energies change. We denote the continuation of these three branches to finite field as 3, 1, and 2, respectively. The field dependence at $k=\pi$ for a field polarized along the x axis, determined from neutron-scattering experiments, is shown in Fig. 1.

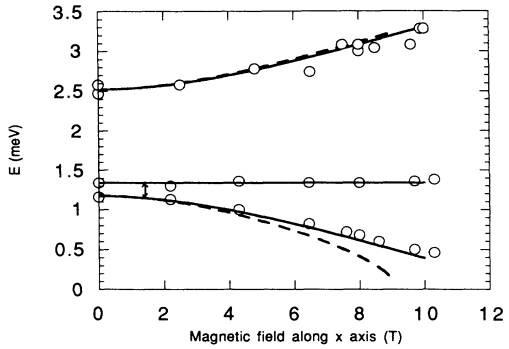

FIG. 1. Field dependence of magnon energies at $k=\pi$ for field oriented along x (i.e., c) axis. Dashed line is boson theory, solid line is fermion theory, and circles are experimental data (Ref. 6). The 47-GHz transition is marked.

The observed ESR signal results from transitions between the 1 and 2 branches. Transitions will occur at values of field and wave vector satisfying

$$|E_1(k,H) - E_2(k,H)| = \omega\hbar, \quad (7)$$

where $\omega = 47$ GHz is the microwave frequency. With anisotropy present, $E_1(k,H)-E_2(k,H)$ depends on k. This has the effect of broadening the resonance. Equation (5) is now replaced by

$$2\hbar\chi''(\omega) = L\hbar(1-e^{-\omega\hbar/T})\int dk\, e^{-E_{\min}(k,H)/T}|\langle k,2|\mathcal{S}^z|k,1\rangle|^2\delta[|E_1(k,H)-E_2(k,H)|-\omega\hbar], \quad (8)$$

where

$$E_{\min} \equiv \min\{E_1, E_2\}. \quad (9)$$

For some range of H the δ-function constraint can be satisfied at some value of $k=k_0$ giving

$$2\hbar\chi''(\omega) = L\hbar(1-e^{-\omega\hbar/T})e^{-E_{\min}(k_0,H)/T}|\partial E_1(k_0,H)/\partial k - \partial E_2(k_0,H)/\partial k|^{-1}|\langle k_0,2|\mathcal{S}^z|k_0,1\rangle|^2. \quad (10)$$

It can happen that the δ-function constraint is satisfied for several values of k; in that case we obtain a sum of terms of the above type. We expect $E_{1,2}(k,H)$ to be differentiable functions of $(k-\pi)^2$. It then follows that the Jacobian factor in the above equation blows up at the value of H $(=H_0)$ for which $k_0(H_0)=\pi$, due to the diverging density of states. This divergence should be proportional to $|H-H_0|^{-1/2}$ and would be smoothed out by three-dimensional effects. After integration over H, the intensity is finite. Thus the peak field is determined by the field dependence of the energies at $k=\pi$ only. This has been measured in neutron-scattering experiments for one relevant orientation of the field: parallel to the x (i.e., c) axis. To proceed, we need to know the wave vector and field-dependent dispersion relations $E_{1,2}(k,H)$ and the above matrix element. These are not known from any exact theory and have been only partially determined experimentally. Thus we must adopt an approximate model. (Alternatively, finite-lattice diagonalization or Monte Carlo could be used.)

At least three different field-theory approximations have been introduced to study Haldane-gap antiferromagnets of spin s. The original one introduced by Haldane[1] is the $O(3)$ nonlinear σ model. This becomes exact at large s (in the low-energy limit) but has the disadvantage that very little can be exactly calculated using it; in particular the field-dependent magnon energies in the presence of anisotropy have not been calculated. The simplest field theory is the Landau-Ginsburg model[8,9] where a three-component bosonic field is introduced with

a quartic potential and is treated in the Gaussian approximation. This essentially arises in the large-n limit of the $O(n)$ nonlinear σ model. It also becomes exact, in some cases, near the critical interchain coupling that produces three-dimensional Néel order. A third approximation[10] involves a triplet of massive, free, Majorana fermions. This becomes exact for the spin-one bilinear-biquadratic Hamiltonian when the ratio of couplings approaches -1 at which point the gap vanishes, the model becomes Bethe ansatz integrable, and a transition to a dimerized phase occurs.[11] Note that, at temperatures much less than the gap, we may use Boltzman statistics so that the difference between fermions and bosons becomes unobservable by most experimental probes. Recent neutron-scattering experiments[6] suggest that the third model is much more successful than the second at predicting the field dependence of magnon energies. We will apply both models to the ESR calculation. While both are in fair agreement with the data on resonance fields, the Landau-Ginsburg model agrees better. This suggests that it may give the field dependence of magnon energies more accurately at low fields (<5 T) for arbitrary orientation. Again, we emphasize that this could be checked by further neutron-scattering experiments.

The Landau-Ginsburg model is described by the Lagrangian

$$\mathcal{L}=(1/2v)|\partial\boldsymbol{\phi}/\partial t+g\mu_B\mathbf{H}\times\boldsymbol{\phi}|^2 -(v/2)(\partial\boldsymbol{\phi}/\partial x)^2-(1/2v)\sum_i \Delta_i^2\phi_i^2 . \tag{11}$$

Here $\boldsymbol{\phi}$ is a three-component vector representing the long-wavelength staggered magnetization field. The uniform magnetization density is given by $(g\mu_B/v)\boldsymbol{\phi}\times\partial\boldsymbol{\phi}/\partial t$. The phenomenological parameters Δ_i represent the gaps of the three branches of magnons at zero field. A $\boldsymbol{\phi}^4$ term is generally added for stability, but it will not be needed for the present discussion, since we only consider fields below the critical field. The field $\boldsymbol{\phi}$ can be expanded in magnon creation and annihilation operators

$$\boldsymbol{\phi}(x,t)=\int\frac{dk}{4\pi\omega_k}[e^{-i(\omega t-kx)}\mathbf{a}_k+e^{i(\omega t-kx)}\mathbf{a}_k^\dagger] . \tag{12}$$

Thus we see that the uniform magnetization field $(g\mu_B/v)\boldsymbol{\phi}\times\partial\boldsymbol{\phi}/\partial t$ is quadratic in magnon creation and annihilation operators. There are two types of terms. The first type annihilates or creates a pair of magnons. These terms contribute to the susceptibility only at frequencies greater than twice the gap. They are responsible for the zero-temperature neutron-scattering cross section near zero wave vector.[12] The second type of term contains both an annihilation and a creation operator, of different polarizations. Thus it is a magnon spin-flip operator. It contributes to the susceptibility at lower frequencies, above the minimum *difference* of gaps, but only at finite temperatures where a thermal population of magnons is present. It is this type of term with which we are presently concerned. We take the magnetic field to lie in the 1-2 plane

$$\mathbf{H}=(H_1,H_2,0),\quad H\equiv\sqrt{H_1^2+H_2^2} . \tag{13}$$

The Euler-Lagrange equations

$$(d/dt)\partial\mathcal{L}\partial\dot{\phi}^a=\partial\mathcal{L}\partial\phi^a \tag{14}$$

give, in a Fourier transformed representation

$$\begin{pmatrix} \omega^2-v^2k^2-\Delta_1^2+(g\mu_BH_2)^2 & -(g\mu_B)^2H_1H_2 & 2i\omega g\mu_BH_2 \\ -(g\mu_B)^2H_1H_2 & \omega^2-v^2k^2-\Delta_2^2+(g\mu_BH_1)^2 & -2i\omega g\mu_BH_1 \\ -2i\omega g\mu_BH_2 & 2i\omega g\mu_BH_1 & \omega^2-v^2k^2-\Delta_3^2+(g\mu_BH)^2 \end{pmatrix}\boldsymbol{\phi}=0 . \tag{15}$$

Here ω and k represent the frequency and wave vector *(shifted by π)* of the magnon. By setting the determinant of the above matrix to zero we obtain a cubic equation in ω^2:

$$\omega^6+a_1\omega^4+a_2\omega^2+a_3=0 , \tag{16}$$

where the coefficients are given by

$$a_1=-\Delta_1^2-\Delta_2^2-\Delta_3^2-3v^2k^2-2(g\mu_BH)^2 ,$$

$$a_2=[\Delta_1^2+v^2k^2-(g\mu_BH_2)^2][\Delta_2^2+v^2k^2-(g\mu_BH_1)^2]+[\Delta_3^2+v^2k^2-(g\mu_BH)^2] \times[\Delta_1^2+\Delta_2^2+2v^2k^2-(g\mu_BH)^2]+4(\Delta_1^2+v^2k^2)(g\mu_BH_1)^2+4(\Delta_2^2+v^2k^2)(g\mu_BH_2)^2 , \tag{17}$$

$$a_3=-[\Delta_1^2+v^2k^2-(g\mu_BH_2)^2][\Delta_2^2+v^2k^2-(g\mu_BH_1)^2][\Delta_3^2+v^2k^2-(g\mu_BH)^2] +(g\mu_B)^4H_1^2H_2^2[\Delta_3^2+v^2k^2-(g\mu_BH)^2] .$$

In the special case $H_2=0$, the dispersion relation of the first magnon branch is unaffected by the field H_1, which mixes only the second and third branches, as reported earlier:[9]

$$\omega_1^2=\Delta_1^2+v^2k^2 ,$$
$$\omega_{3,2}^2=(\Delta_2^2+\Delta_3^2+2v^2k^2)/2+(g\mu_BH)^2 \pm[2(g\mu_BH)^2(\Delta_2^2+\Delta_3^2+2v^2k^2)+(\Delta_2^2-\Delta_3^2)^2/4]^{1/2} . \quad (18)$$

This formula, with $k=0$, is compared with the recent neutron-scattering measurements in Fig. 1 using the parameters $g=2.2$, $\Delta_3=2.52$ meV, $\Delta_1=1.34$ meV, and $\Delta_2=1.17$ meV. [The theoretical curve differs from the corresponding one in Ref. 6 only in that we have used unequal values of Δ_1 and Δ_2.] While the agreement of theory and experiment is quite good up to $h=5$ T, it is rather bad at larger fields; in particular, the critical field at which the gap vanishes $H_{2c}=\Delta_1/g\mu_B$ is about 30% too low. The above formula may also be applied in the case where the field is in the three direction, by the replacement, $\Delta_3\rightarrow\Delta_1$. This is compared to experiment in Fig. 2. [Again the difference with Ref. 6 is only the use of unequal values of Δ_1 and Δ_2.] Likewise, this formula may be used when the field is along the 2 axis, the result being shown in Fig. 3. Note the level crossing that occurs, since the first and second branches don't mix. This is probably an artifact of the Gaussian approximation. Magnon-interaction effects, modeled by the ϕ^4 term in the Landau-Ginsburg approach, should mix these modes and produce level repulsion. We now consider the case where the field lies in the 1-2 plane but not along one of the axes. In this case all three branches are mixed. The solutions of the general cubic equation, Eq. (16), can be expressed in terms of

$$Q\equiv(a_1^2-3a_2^2)/9 ,$$
$$R\equiv(2a_1^3-9a_1a_2+27a_3)/54 , \quad (19)$$
$$T\equiv\arccos(R/Q^{3/2}) ,$$

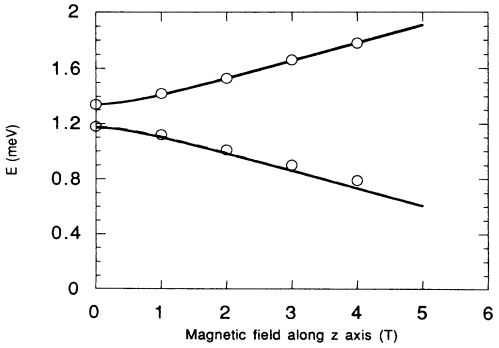

FIG. 2. Field dependence of magnon energies at $k=\pi$ for field oriented along z (i.e, b) axis. Dashed line is boson theory, solid line is fermion theory, and circles are experimental data (Ref. 6). (The two theories are essentially indistinguishable in this case.)

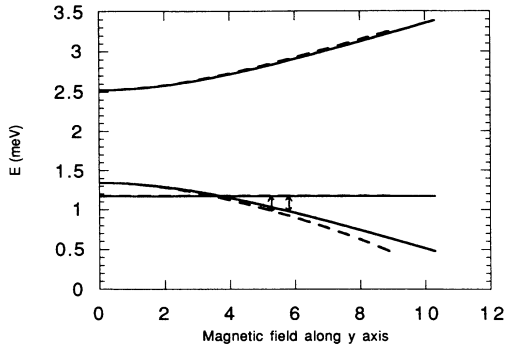

FIG. 3. Field dependence of magnon energies at $k=\pi$ for field oriented along y (i.e., a) axis. Dashed line is boson theory, solid line is fermion theory. 47-GHz transitions are marked. Magnon interaction effects, not taken into account in producing these curves, are expected to eliminate the level crossing shown here.

as

$$\omega_1^2=-2\sqrt{Q}\cos[(T+2\pi)/3]-a_1/3 ,$$
$$\omega_2^2=-2\sqrt{Q}\cos[T/3]-a_1/3 , \quad (20)$$
$$\omega_3^2=-2\sqrt{Q}\cos[(T+4\pi)/3]-a_1/3 .$$

The field dependence (at $k=0$) is shown for the case where the field makes a 60° angle with the x axis, in Fig. 4. Note that all three branches are now field dependent.

The magnon polarization is also given by Eq. (15). Consider, for example the case where the field is along the x axis. Then the 1 mode is polarized in the x direction, i.e., it couples only to $\langle S^x(k,\omega)S^x(-k,-\omega)\rangle$. On the other hand, the 2 and 3 branches have linear combinations of y and z polarization, given by the solutions of Eq. (15), which can be written in the form $\phi_2=(0,\cos\phi,i\sin\phi)$ and $\phi_3=(0,i\sin\phi,\cos\phi)$. The angle ϕ gives the polarization in the yz plane, measured from the y (z) axis for the second (third) branch. The factor of i signifies that the y and z components of the magnon wave function are out of phase. The polarization angle ϕ is given by

$$\tan\phi=2\omega_3(H)g\mu_BH/[\omega_3(H)^2-\Delta_2^2+(g\mu_BH)^2] , \quad (21)$$

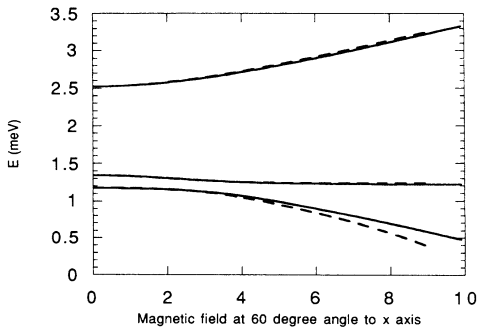

FIG. 4. Field dependence of magnon energies at $k=\pi$ for field at 60° angle to x axis in x-y plane. Dashed line is boson theory, solid line is fermion theory.

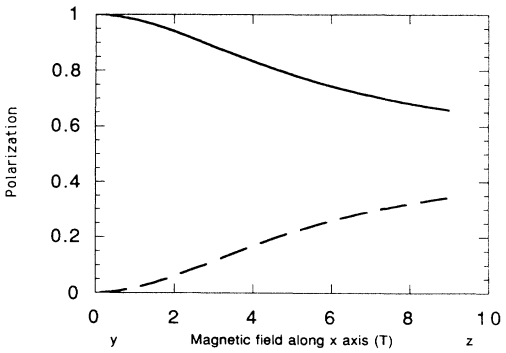

FIG. 5. Polarization of second and third magnon branches at $k=\pi$ for field along x axis, $\cos^2\phi$, $\sin^2\phi$ as defined in Eq. (21). Solid (dotted) lines are second (third) branch. At zero field, the second (third) branch has pure $y(z)$ polarization.

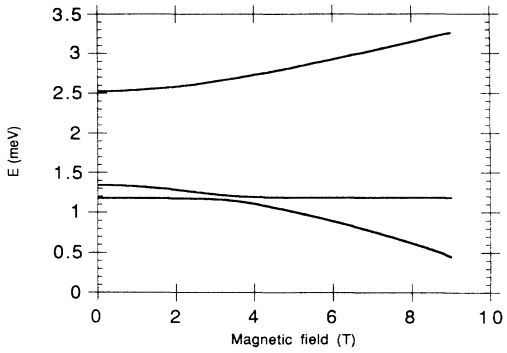

FIG. 7. Field dependence of magnon energies at $k=\pi$ for field at 80° angle to x axis in x-y plane using boson theory. This illustrates qualitatively what curves might look like for a 90° angle if magnon interaction effects were included.

$\cos^2\phi$ and $\sin^2\phi$ are plotted for this case in Fig. 5.

The ESR resonance frequencies can be deduced immediately. For a field applied in the 1-2 plane, a 47-GHz transition occurs between branches 1 and 2 for a field in the range 1.4–5.3 T. These transitions are marked in Figs. 1 and 3. A plot of resonance field vs field orientation is shown in Fig. 6, comparing theory and experiment. Note that the agreement between theory and experiment is excellent when the field is oriented in the x direction. This is no surprise because the theoretical magnon frequencies agree with the neutron-scattering measurements (Fig. 1) for this orientation and field. On the other hand, the theoretical resonance field is about 6% too high for the field along the y axis. This is also not surprising. We see from Fig. 3 that, according to the Landau-Ginsburg model in Gaussian approximation, the ESR transition occurs at a sufficiently large field that branches 1 and 2 have crossed and then separated by 47 GHz. However, we expect magnon-interaction effects to mix branch 1 and 2, producing level repulsion. This would likely have the effect of producing a 47-GHz splitting of the two branches at a lower field (presumably still greater than the field of closest approach). This effect could be calculated perturbatively in the ϕ^4 interaction in the Landau-Ginsburg model. We illustrate the field-dependent energies that might occur in Fig. 7. (This is actually the prediction of the noninteracting theory for the field at an angle of 81° to the x axis.)

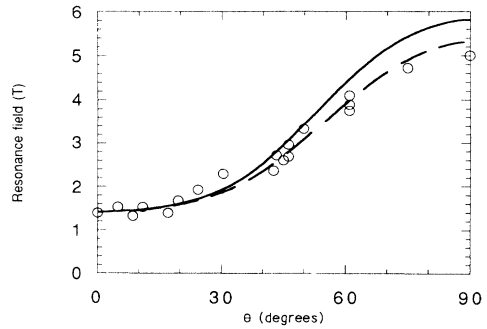

FIG. 6. ESR resonance field vs orientation of field in x-y plane. θ is the angle measured from the x axis. Dashed line is boson theory, solid line is fermion theory, and circles are experimental data (Ref. 4).

Alternatively, we may apply the fermion field theory[10] to the problem. In this model, the three free massive bosons are replaced by three free massive fermions of Majorana type (i.e., there is no antiparticle). The Lagrangian density becomes

$$\mathcal{L}=\psi_L i\cdot\partial_-\psi_L+\psi_R i\cdot\partial_+\psi_R +i\sum_i \Delta_i(\psi_{Li}\psi_{Ri}-\psi_{Ri}\psi_{Li}) +ig\mu_B\mathbf{H}\cdot(\psi_L\times\psi_L+\psi_R\times\psi_R)\ , \tag{22}$$

where

$$\partial_\pm\equiv\partial_t\pm v\partial_x\ , \tag{23}$$

and $\psi_{L,R}$ are left (right) -moving fermion fields. The uniform magnetization density is quadratic in fermion fields

$$ig\mu_B(\psi_L\times\psi_L+\psi_R\times\psi_R)\ .$$

Thus it contains magnon spin-flip terms just as in the case of the Landau-Ginsburg model. (On the other hand, the staggered magnetization has a rathered complicated representation in this model. It is not local in the Fermion fields.[10]) It is convenient to combine ψ_L and ψ_R into a six-dimensional vector and to define a 3×3 diagonal matrix

$$\Delta\equiv\begin{bmatrix}\Delta_1&0&0\\0&\Delta_2&0\\0&0&\Delta_3\end{bmatrix}\ . \tag{24}$$

After Fourier transforming, the Euler-Lagrange equations become

$$\begin{bmatrix}\omega-vk+g\mu_B\mathbf{H}\times & i\Delta\\ -i\Delta & \omega+vk+g\mu_B\mathbf{H}\times\end{bmatrix}\begin{bmatrix}\psi_L\\\psi_R\end{bmatrix}=0\ . \tag{25}$$

Setting the determinant of the above 6×6 matrix to zero gives, after some algebra, a cubic equation in ω^2, as in Eq. (16) with coefficients

$$a_1=-\Delta_1^2-\Delta_2^2-\Delta_3^2-2(g\mu_B H)^2-3v^2k^2\ ,$$
$$a_2=\Delta_1^2\Delta_2^2+\Delta_1^2\Delta_3^2+\Delta_2^2\Delta_3^2+2(g\mu_B H_1)^2(\Delta_1^2-\Delta_2\Delta_3)+2(g\mu_B H_2)^2(\Delta_2^2-\Delta_1\Delta_3)$$
$$+(g\mu_B H)^4+2v^2k^2(\Delta_1^2+\Delta_2^2+\Delta_3^2)+3v^4k^4\ , \tag{26}$$

$$a_3=-\Delta_1^2\Delta_2^2\Delta_3^2+2(g\mu_B H_1)^2\Delta_1^2\Delta_2\Delta_3+2(g\mu_B H_2)^2\Delta_2^2\Delta_1\Delta_3-(g\mu_B H_1)^4\Delta_1^2$$
$$-(g\mu_B H_2)^4\Delta_2^2-2(g\mu_B H_1)^2(g\mu_B H_2)^2\Delta_1\Delta_2$$
$$+v^2k^2[-\Delta_1^2\Delta_2^2-\Delta_2^2\Delta_3^2-\Delta_2^2\Delta_3^2+2(g\mu_B H_1)^2(\Delta_1^2+\Delta_2\Delta_3)+2(g\mu_B H_2)^2(\Delta_2^2+\Delta_1\Delta_3)-(g\mu_B H)^4]$$
$$+(vk)^4[-\Delta_1^2-\Delta_2^2-\Delta_3^2+2(g\mu_B H)^2]-(vk)^6\ .$$

Again, when the field is along one of the symmetry axes that branch is unaffected. Choosing the field to lie along the x axis, we obtain

$$\omega_1^2=\Delta_1^2+v^2k^2$$
$$\omega_{3,2}^2=(\Delta_2^2+\Delta_3^2+2v^2k^2)/2+(g\mu_B H)^2$$
$$\pm\{(g\mu_B H)^2[(\Delta_2+\Delta_3)^2+4v^2k^2]$$
$$+(\Delta_2^2-\Delta_3^2)^2/4\}^{1/2}\ , \tag{27}$$

as found previously.[10] This formula was used to generate the "fermion" theoretical curves in Figs. (1)–(3). We see from Fig. 1 that the fermion theory fits the experimental data much better than the boson theory at fields larger than about 5 T. When the field is not along a symmetry axis all three branches mix as illustrated in Fig. 4. The corresponding ESR field is shown in Fig. 6, as a function of angle. In this case we see that the boson theory gives a better fit.

We may also calculate the ESR intensity as a function of field using either model. We see from Eq. (10) that the intensity is given by a product of a Boltzman factor, a Jocobian, and a matrix element. Since the Hamiltonian is quadratic, the calculation of the matrix elements in Eq. (10) follows straightforwardly from the eigenvectors determined by Eq. (15) or (25). In any event, most of the field dependence comes from the first two factors. The second factor gives a square root divergence at the field corresponding to zero-momentum magnons. We found that the intensity generally has an asymmetric shape as shown in Fig. 8 for a field oriented along the x axis and a temperature of 3 K, using the fermion theory. In this case, half the integrated intensity lies within about .1 T of the peak. Similar results are obtained for other orientations using either model. The experimental intensity curve given in Ref. 4 (for a different field orientation) is much broader, about 1 T in width, and symmetric. Some kind of disorder in the NENP crystals may play a role in this broadening. Likewise, it is difficult to understand the temperature dependence in detail, using these models. They predict an essentially exponential temperature dependence of the form $e^{-E_{\min}/T}$ with $E_{\min}\approx\Delta_2\approx 14$ K. The experimental data does not show a decrease until T is lowered to about 5 K. Below this temperature there *is* a rapid decrease, which could be consistent with exponential behavior but would correspond to a considerably smaller gap of about 5 K.

In conclusion, we have argued that ESR experiments at temperatures well below the Haldane gap measure transitions between different magnon branches of wave vector near π, split by crystal-field anisotropy and magnetic field. It is unnecessary to postulate any additional excitations beyond the magnons observed in neutron-scattering experiments. This picture is in excellent agreement with neutron-scattering data on field-dependent magnon energies where they are available and in fair agreement with field-theory models in all cases. More neutron-scattering experiments with other field orientations could help to confirm this picture. In particular, applying the field along the y (i.e., c) axis, the ESR experiment implies that the separation of the lowest two branches should be 47 GHz (0.19 meV) at a field of 5 T. Such a measurement would also probe magnon interaction effects, which should lead to mixing of branches 1 and 2.

For the isotropic Heisenberg model the ESR intensity follows exactly from simple symmetry considerations and the assumed triplet excitation. Including crystal-field anisotropy the field dependence of the magnon spectrum and the matrix elements of Eq. (10) become model dependent. We have calculated them using two exactly solvable models, with Hamiltonians quadratic in boson or fermion fields, respectively. We expect these models to contain at least all the qualitative properties of the problem. It is important to realize that the field-dependent spectrum can be measured independently from neutron scattering, testing both the models and the consistency with ESR experiments. We don't expect that use of a

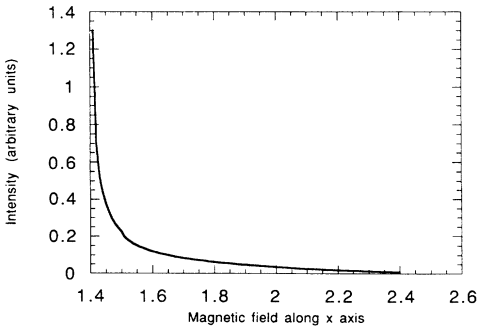

FIG. 8. ESR intensity vs field for field oriented along the x axis from the fermion theory.

more exact model (i.e., numerical work on the Heisenberg Hamiltonian including crystal-field terms) would lead to major changes to the results of these models, apart from the level repulsion effect discussed above. While it is possible that this would resolve the discrepancy in the line width and temperature dependence, we suspect that these are more likely the result of impurities or other nonintrinsic effects.

Note added in proof. The same interpretation of the ESR data of Ref. 4 has been given independently by L. C. Brunel *et al.* (unpublished) and supported by additional experiments by that group and by W. Palme *et al.* (unpublished). The latter work finds a temperature dependence consistent with that predicted here. More recent experiments [J. P. Boucher (private communication)] obtain an intensity curve that is narrower by about a factor of 10 than that of Ref. 4, consistent with that predicted here.

I would like to thank Stan Geshwind for encouraging me to complete these calculations and Walter Hardy for a helpful discussion.

[1]F. D. M. Haldane, Phys. Lett. **93A**, 464 (1983). For a review see I. Affleck, J. Phys.: Condens. Matter **1**, 3047 (1989).

[2]W. J. L. Buyers, R. M. Morra, R. L. Armstrong, P. Gerlach, and K. Hirakawa, Phys. Rev. Lett. **56**, 371 (1986).

[3]J.-P. Renard, M. Verdaguer, L. P. Regnault, W. A. C. Erkelens, J. Rossat-Mignod, and W. G. Stirling, Europhys. Lett. **3**, 945 (1987); J.-P. Renard, M. Verdaguer, L. P. Regnault, W. A. C. Erkelens, J. Rossat-Mignod, J. Ribad, W. G. Stirling, and C. Vettier, J. Appl. Phys. **63**, 3538 (1988).

[4]M. Date and K. Kindo, Phys. Rev. Lett. **65**, 1659 (1990).

[5]M. Hagiwara, K. Katsumata, I. Affleck, B. I. Halperin, and J.-P. Renard, Phys. Rev. Lett. **65**, 3181 (1990); S. J. Glarum, S. Geschwind, K. M. Lee, M. L. Kaplan, and J. Michel, Phys. Rev. Lett. **67**, 1614 (1991).

[6]L. P. Regnault, C. Vettier, J. Rossat-Mignod, and J.-P. Renard, J. Magn. Magn. Mater. **104-107**, 869 (1992).

[7]M. Takahashi, Phys. Rev. Lett. **62**, 2313 (1989).

[8]I. Affleck, Phys. Rev. Lett. **62**, 474 (1989); **65**, 2477(E) (1990); **65**, 2835(E) (1990).

[9]I. Affleck, Phys. Rev. B **41**, 6697 (1990).

[10]A. M. Tsvelik, Phys. Rev. B **42**, 10499 (1990).

[11]I. Affleck and F. D. M. Haldane, Phys. Rev. B **36**, 5291 (1987).

[12]I. Affleck and R. A. Weston, Phys. Rev. B **45**, 4667 (1992).